Modeling Internal Solitary Waves in the Coastal Ocean

Roger Grimshaw[1], Efim Pelinovsky[2] and Tatiana Talipova[2]

[1] Department of Mathematical Sciences, Loughborough University, UK

[2] Institute of Applied Physics, Nizhny Novgorod, Russia

December 18, 2006

Abstract

In the coastal oceans, the interaction of currents (such as the barotropic tide) with topography can generate large-amplitude, horizontally propagating internal solitary waves. These waves often occur in regions where the waveguide properties vary in the direction of propagation. We consider the modeling of these waves by nonlinear evolution equations of the Korteweg-de Vries type with variable coefficients, and we describe how these models to describe the shoaling of internal solitary waves over the continental shelf and slope. The theories are compared with various numerical simulations.

1 Introduction: Variable-coefficient Korteweg-de Vries equation

Solitary waves are nonlinear waves of permanent form, first observed by Russell (1844) in a now famous report on his observations of a free surface solitary wave in a canal, and his subsequent experiments. Later, theoretical work by Boussinesq (1871) and Rayleigh (1876) confirmed Russell's findings, and then Korteweg and de Vries (1895) derived their well-known equation, which contains the solitary wave as one of its principal solutions. But it was not until the second half of the twentieth century that it was realised

that the Korteweg-de Vries (KdV) equation, as well as being a notable integrable equation, was also a valid model for solitary waves in a wide variety of physical contexts. Of principal concern here are the large-amplitude internal solitary waves which propagate in the coastal oceans (for recent reviews see , e.g., Apel (1995), Grimshaw (2001) and Holloway et al (2001)). They owe their existence to a balance between nonlinear wave-steepening effects and linear wave dispersion, and hence can be effectively modeled by nonlinear evolution equations of the KdV-type.

Many studies based on KdV-type models have used equations with constant coefficents. Beginning with seminal paper by Benney (1966) there have been derivations of a (constant-coefficient) KdV equation suitable for the description of internal solitary waves, see, for instance, Lee and Beardsley (1974), Ostrovsky (1978), Maslowe and Redekopp (1980), Grimshaw (1981), Tung *et al* (1981)), and the recent articles by Holloway et al (1997, 1999, 2001), Grimshaw (2001, 2005), Grimshaw et al (2006) and Helfrich and Melville (2006)) which review the literature in this area. However, in the present oceanic framework, the waves are propagating on a background whose properties vary in the wave propagation direction. In this situation, an appropriate model equation is the variable-coefficient KdV equation

$$A_t + cA_x + \frac{cQ_x}{2Q}A + \mu AA_x + \delta A_{xxx} + \nu A = 0\,, \tag{1}$$

Here $A(x,t)$ is the amplitude of the wave, and x, t are space and time variables respectively. The coefficient $c(x)$ is the relevant linear long wave speed, and $Q(x)$ is the linear magnification factor, defined so that QA^2 is the wave action flux density for linear long waves. The coefficients μ and δ of the nonlinear and dispersive terms respectively are determined by the waveguide properties of the specific physical system being considered, and they are functions of x. The final term νA represents nonconservative effects arising from dissipative or forcing terms in the underlying basic state. Extra terms can also be added to represent dissipative effects on the wave itself (see Grimshaw et al (2003)), and Coriolis effects due to the Earth's rotation (see Grimshaw et al (1998b, 2006)) , but these will not be considered here. The variable-coefficient KdV equation for water waves was developed by Ostrovsky and Pelinovsky (1970) and later systematically derived by Johnson(1973b), while Grimshaw (1981) gave a detailed derivation for internal waves (see also Zhou and Grimshaw(1989) and Grimshaw (2001)). The derivation assumes the usual KdV balance that the amplitude η has the same order as the dispersion,

measured by $\partial^2/\partial x^2$, and in addition assumes that the waveguide properties (i.e. the coefficients c, Q, μ, δ) vary slowly so that Q_x/Q for instance is of the same order as the dispersion. In this scenario, the first two terms in (1) are the dominant terms, and hence we make the transformation

$$U = \sqrt{Q}\, A\,, \quad \tau = \int^x \frac{dx}{c}\,, \quad \xi = \tau - t\,. \tag{2}$$

Substitution into (1) yields, to the same order of approximation as in the derivation of (1),

$$U_\tau + \alpha U U_\xi + \lambda U_{\xi\xi\xi} + \nu U = 0 \tag{3}$$

$$\alpha = \frac{\mu}{c\sqrt{Q}}\,, \quad \lambda = \frac{\delta}{c^3}\,. \tag{4}$$

The coefficients α, λ are functions of τ alone. Note that although τ is a variable along the spatial path of the wave, we shall subsequently refer to it as the "time". Similarly, although ξ is a temporal variable (in a reference frame moving with speed c), we shall subsequently refer to it as a "space" variable. We shall call equation (3) the vKdV equation.

In this paper, we shall review the theory of slowly-varying solitary waves based on the variable-coefficient Korteweg-de Vries equation (3) in Section 2. But because internal solitary waves are often of large amplitudes, it is sometimes useful to include a cubic nonlinear term in (1) and (3), which then become respectively (see the review by Grimshaw 2001),

$$A_t + cA_x + \frac{cQ_x}{2Q}A + \mu A A_x + \mu_1 A^2 A_x + \delta A_{xxx} + \nu A = 0\,, \tag{5}$$

$$U_\tau + \alpha U U_\xi + \beta U^2 U_\xi + \lambda U_{\xi\xi\xi} + \nu U = 0\,, \tag{6}$$

$$\text{where} \quad \beta = \frac{\mu_1}{cQ}\,. \tag{7}$$

Equations (3, 6), sometimes with various modifications such as with an additional dissipative term, or with a term taking account of the earth's rotation, have been applied to the study of internal solitary wave wave transformation in the coastal zone by many authors (for instance Cai et al. (2002), Djordjevic and Redekopp (1978), Grimshaw et al (2004, 2006), Holloway et al (1997, 1999), Hsu et al (2000), Liu et al (1988, 1998, 2004), Orr and Mignerey (2003) and Small (2001a,b, 2003),

In Section 3, we shall describe the slowly-varying solitary wave solutions of the vKdV equation (3) and of the extended vKdV equation (6), and in

particular examine in Section 4 the behaviour at certain critical points where either α or β vanish. Then in Section 5 we shall indicate how these theoretical results can be applied for realistic oceanic conditions, and in this context we will show world maps of the coefficients of the extended vKdV equation (3) However, before proceeding to the main body of this paper, we shall present in Section 2 a brief account of the derivation of the KdV equation for internal solitary waves.

2 Derivation of the Korteweg-de Vries equation for internal solitary waves

Here we shall give an outline of the derivation of the KdV equation for surface and internal waves (a more complete discussion and further references can be found in the articles by Holloway et al (1997, 1999, 2001), Grimshaw (2001) and Grimshaw et al (2006), on which this present account is based). For simplicity we suppose first that the waveguide does not vary in the wave propagation direction. Consider then an inviscid, incompressible fluid which is bounded above by a free surface and below by a rigid boundary. We shall suppose that the flow is two-dimensional and can be described by the spatial coordinates (x, z) where x is horizontal and z is vertical, so that the free surface is $z = \eta$ and the bottom is $z = -h$ (see Figure 1). The basic equations are then,

$$\rho(u_t + uu_x + wu_z) + p_x = 0\,, \tag{8}$$

$$\rho(w_t + uw_x + ww_z) + p_z + g\rho = 0\,, \tag{9}$$

$$\rho_t + u\rho_x + w\rho_z = 0\,, \tag{10}$$

$$u_x + w_z = 0\,. \tag{11}$$

Here (u, w) are the velocity components, p is the pressure and ρ is the density, while t is the time coordinate. Note that the effect of the earth's rotation has been neglected. The boundary conditions are

$$w = 0 \quad \text{at} \quad z = -h\,, \tag{12}$$

$$p = 0, \quad \text{at} \quad z = \eta\,, \tag{13}$$

$$\eta_t + u\eta_x = w\,, \quad \text{at} \quad z = \eta\,. \tag{14}$$

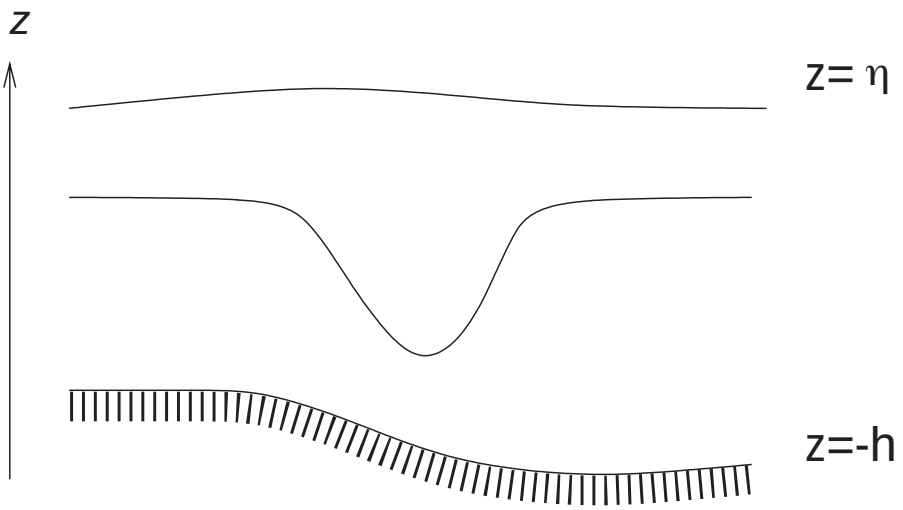

Figure 1: Coordinate system.

In order to develop the multiscale asymptotic procedure which will lead to the KdV equation, it is useful to introduce a small parameter $\epsilon << 1$ to describe the long-wave approximation. Thus we rescale the horizontal coordinate and time,

$$X = \epsilon x\,, \quad T = \epsilon t\,, \tag{15}$$

and then assume that all variables depend on (X, T, z). It follows that we must also the replace w with ϵw.

In the basic state the fluid has a density $\rho_0(z)$, a horizontal shear flow $u_0(z)$ in the $x-$direction, and a pressure field $p_0(z)$. This basic state satisfies the equations (8, 9, 10, 11), and the boundary conditions (12, 13, 14) The density stratification is described by the buoyancy frequency $N(z)$, where

$$N^2(z) = -\frac{g\rho_{0z}}{\rho_0}\,. \tag{16}$$

We shall proceed to obtain the KdV equation for internal solitary waves, but note that to recover the theory for water waves from this general formulation it is sufficient just to put the density $\rho_0(z) =$ constant and (for simplicity) $u_0(z) = 0$ as well. To describe internal solitary waves we seek solutions whose horizontal length scales are much greater than h, and whose

time scales are much greater than N^{-1}. We shall also assume that the waves have small amplitude, characterised by the parameter $\alpha << 1$. It is useful to define an auxiliary variable, ζ the vertical isopycnal displacement from the basic state, defined by the equation $\rho(z,x,t) = \rho_0(z-\zeta,x)$. Thus we seek an expansion in which

$$\rho = \rho_0 + \alpha\rho_1 + \alpha^2\rho_2 + \cdots\,, \tag{17}$$

with similar expansions for all other variables. Linear long wave theory is obtained at the leading order and has solutions in the separable form

$$g\rho_1 = \rho_0 N^2\zeta_1\,, \quad \zeta_1 = A(\theta,S)\phi(z,\tau)\,, \tag{18}$$

$$\text{where} \quad S = \epsilon^2 T = \epsilon^3 t \quad \theta = X - cT = \epsilon(x-ct)\,. \tag{19}$$

The expression for the amplitude A ensures that

$$A_T + cA_X = \epsilon^2 A_S\,. \tag{20}$$

The remaining dependent variables are given by

$$u_1 = A((c-u_0)\phi)_z\,, \quad w_1 = -\frac{A_\theta}{c}(c-u_0)\phi\,, \quad p_1 = \rho_0(c-u_0)^2 A\phi_z\,, \tag{21}$$

Here c is the linear long wave speed, and the modal functions $\phi(z)$ are defined by the boundary-value problem,

$$\{\rho_0(c-u_0)^2\phi_z\}_z + \rho_0 N^2\phi \;=\; 0\,, \quad \text{for} \quad -h < z < \eta_0, \tag{22}$$

$$\phi = 0 \quad \text{at} \quad z = -h\,, \quad (c-u_0)^2\phi_z \;=\; g\phi \quad \text{at} \quad z = \eta_0\,. \tag{23}$$

Typically, the boundary-value problem (22, 23) defines an infinite sequence of modes, $\phi_n^{\pm}(z)$, $n = 0,1,2,\ldots$, with corresponding speeds $c_n^{\pm}$. Here, the superscript "$\pm$" indicates waves with $c_n^+ > u_M = \max u_0$ and $c_n^- < u_M = \min u_0$ respectively. We shall confine our attention to these regular modes, and consider only stable shear flows. Nevertheless, we note that there may also exist singular modes with $u_m < c < u_M$ for which an analogous theory can be developed (Maslowe and Redekopp, 1980). Note that it is useful to let $n = 0$ denote the surface gravity waves for which c scales with $\sqrt{gh}$, and then $n = 1,2,3,\ldots$ denotes the internal gravity waves for which c scales with Nh. In general, the boundary-value problem (22, 23) is readily solved numerically. Typically, the surface mode ϕ_0 has no extrema

in the interior of the fluid and takes its maximum value at the surface $z = 0$, while the internal modes $\phi_n^{\pm}(z)$, $n = 1, 2, 3, \ldots$, have n extremal points in the interior of the fluid, and vanish near $z = 0$ (and, of course, also at $z = -h$). Since the modal equations are homogeneous, we are free to impose a normalization condition on $\phi(z)$. A commonly used condition is that $\phi(z_m) = 1$ where $|\phi(z)|$ achieves a maximum value at $z = z_m$ with respect to z. In this case the amplitude αA is uniquely defined as the amplitude of $\zeta^{1)}$ at z_m.

It can now be shown that, within the context of linear long wave theory, any localised initial disturbance will evolve into a set of outwardly propagating modes, each given by an expression of the form (18). Assuming thats the speeds $c_n^{\pm}$ of each mode are sufficiently distinct, it is sufficient for large times to consider just a single mode. Henceforth, we shall omit the indices and assume that the mode has speed c, amplitude $A(\theta, S)$ and modal function $\phi(z)$. Then, as time increases, the hitherto neglected nonlinear terms begin to have an effect, and cause wave steepening. However, this is opposed by the terms representing linear wave dispersion, also neglected in the linear long wave theory. A balance between these effects emerges as time increases and the outcome is the KdV equation for the wave amplitude. These processes are enforced by imposing the KdV balance

$$\alpha = \epsilon^2 \,. \tag{24}$$

Then, in the expansion (17) this process is formally determined at the next order, where the equation for ζ_2 is,

$$\{\rho_0(c-u_0)^2\zeta_{2Xz}\}_z + \rho_0 N^2 \zeta_{2X} = M_2 \,, \quad \text{for} \quad -h < z < \zeta_0 \tag{25}$$

$$\zeta_{2X} = 0 \quad \text{at} \quad z = -h \,, \quad \rho_0(c-u_0)^2\zeta_{2Xz} - \rho_0 g \zeta_{2X} = N_2 \,, \quad \text{at} \quad z = \zeta_0 \,. \tag{26}$$

Here the inhomogeneous terms M_2, N_2 are known in terms of $A(X, T)$ and $\phi(z)$, and are given by

$$\begin{aligned} M_2 &= 2\{\rho_0(c-u_0)\phi_z\}_z A_S + 3\{\rho_0(c-u_0)^2\phi_z^2\}_z A A_\theta \\ &\qquad -\rho_0(c-u_0)^2\phi A_{\theta\theta\theta} \,, \end{aligned} \tag{27}$$

$$N_2 = 2\{\rho_0(c-u_0)\phi_z\}A_S + 3\{\rho_0(c-u_0)^2\phi_z^2\}A A_\theta \,. \tag{28}$$

Note that the left-hand side of equations (25, 26)) are identical to the equations defining the modal function (i.e. (22, 23)), and hence these equations can be solved only if a certain compatibility condition is satisfied. The required compatibility condition is that the inhomogenous terms in (25, 26)

should be orthogonal to the solutions of the adjoint of the modal equations (22, 23). This gives

$$\int_{-h}^{\zeta_0} M_2\phi \, dz = [N_2\phi]_{z=\zeta_0} \, . \tag{29}$$

Substituting the expressions (27, 28) into (29) we obtain the required evolution equation for A, namely the KdV equation

$$A_S + \mu A A_\theta + \delta A_{\theta\theta\theta} = 0 \, . \tag{30}$$

Taking into account the scaling (15) this is just (1), reduced to the case of constant coefficients (that is, $Q = 0$), and where here the coefficients μ and δ are given by

$$I\mu = 3\int_{-h}^{0} \rho_0 (c-u_0)^2 \phi_z^3 \, dz \, , \tag{31}$$

$$I\delta = \int_{-h}^{0} \rho_0 (c-u_0)^2 \phi^2 \, dz \, , \tag{32}$$

$$\text{where} \qquad I = 2\int_{-h}^{0} \rho_0 (c-u_0) \phi_z^2 \, dz \, . \tag{33}$$

Note that for a right-going wave (that is $c > u_M$) the coefficient $\delta > 0$, but that μ can take either sign.

Proceeding to the next highest order will yield an equation set analogous to (25, 26) for ζ_3, whose compatibility condition then determines an evolution equation for the second-order amplitude A_2. We shall not give details here, but note that using the transformation $A + \alpha A_2 \to A$, and then combining the KdV equation (30) with the evolution equation for A_2 will lead to a higher-order KdV equation for A,

$$A_S + \mu A A_\theta + \delta A_{\theta\theta\theta}$$

$$+\alpha\{\delta_1 A_{\theta\theta\theta\theta\theta} + \mu_1 A^2 A_\theta + \sigma_1 A A_{\theta\theta\theta} + \sigma_2 A_\theta A_{\theta\theta}\} \, = \, 0 \, .$$

Explicit expresions for the coefficients are given by Gear and Grimshaw (1983), Lamb and Yan (1996), and Grimshaw *et al* (2002)). However, this equation is not unique, as the near-identity transformation $A \to A + \alpha(aA^2 + bA_{\theta\theta})$ asymptotically reproduces the same equation but with altered coefficients,

$$(\delta_1, \mu_1, \sigma_1, \sigma_2) \to (\delta_1, \mu_1 - a\mu, \sigma_1, \sigma_2 - 6a\delta + 2b\mu).$$

Note that to be Hamiltonian, $\sigma_2 = 2\sigma_1$. Further the enhanced transformation

$$A \to A + \alpha(aA^2 + bA_{\theta\theta} + a'A_\theta \int^\theta A\, d\theta + b'\theta A_T)\,,$$

can asymptotically reduce the higher-order equation to the KdV equation provided that $\mu \neq 0, \delta \neq 0$.

A particularly important special case of the higher-order KdV equation arises when the nonlinear coefficient μ (30) in the KdV equation is close to zero. In this situation, the cubic nonlinear term in the higher-order KdV equation is the most important higher-order term. The KdV equation (30) may then be replaced by the extended KdV equation,

$$A_S + \mu A A_\theta + \alpha\mu_1 A^2 A_\theta + \delta A_{\theta\theta\theta} = 0\,. \tag{34}$$

For $\mu \approx 0$, a rescaling is needed and the optimal choice is to assume that μ is $0(\epsilon)$, and then replace A with A/ϵ. In effect the amplitude parameter is ϵ in place of ϵ^2. The coefficient μ_1 of the cubic nonlinear term is given in terms of integrals of the modal function ϕ and the second order correction term χ_2 (see Grimshaw et al (2002) and Poloukhina et al (2002) for details).

The derivation sketched above was for the case of a waveguide with constant properties in the horizontal direction. But, in the oceanic case, the waveguide often varies slowly due to varying depth, and slow variations in the basic state hydrology and background currents. These effects can be formally incorporated into the theory by supposing that the basic state is a function of the slow variable $\chi = \epsilon^2\theta = \epsilon^3 x$. That is, $h = h(\chi)$, $u_0 = u_0(\chi, z)$ with a corresponding vertical velocity field $\epsilon^3 w_0(z, \chi)$, a density field $\rho_0(z, \chi)$ a corresponding pressure field $p_)(\chi, z)$ and a free surface displacement $\eta_0(\chi)$. This basic sate satisfies the full equation set (8 - 14), with the exception of the momentum equations (8, 9) where there are body forces $(\epsilon^3 F_0(\chi, z), \epsilon^6 G_0(\chi, z))$ respectively. That is

$$\begin{aligned}
\rho_0(u_0 u_{0\chi} + w_0 u_{0z}) + p_{0\chi} &= F_0\,, && (35)\\
\epsilon^6\rho_0(u_0 w_{0\chi} + w_0 w_{0z}) + p_{0z} + g\rho_0 &= \epsilon^6 G_0\,, && (36)\\
u_0\rho_{0\chi} + w_0\rho_{0z} &= 0\,, && (37)\\
u_{0\chi} + w_{0z} &= 0\,. && (38)\\
w_0 + u_0 h_\chi &= 0 \quad \text{at} \quad z = -h(\chi)\,, && (39)\\
p_0 &= 0, \quad \text{at} \quad z = \eta_0\,, && (40)\\
u_0\eta_{0\chi} &= w_0\,, \quad \text{at} \quad z = \eta_0\,. && (41)
\end{aligned}$$

With this scaling, the slow background variability enters the asymptotic analysis at the same order as the weak nonlinear and weak dispersive effects. As noted in the Introduction, it is now necessary to replace the variables S, θ with τ, ξ (2), where it is convenient to replace the slow variable χ with τ. An asymptotic analysis analogous to that described above then produces the vKdV equation (1) (Grimshaw (1981) and Zhou and Grimshaw (1989)). Here first note that we again obtain the expressions (18, 21) with the modal system again defined by (22, 23). But now $c = c(\tau)$ and $\phi = \phi(z, \tau)$, where the τ-dependence is parametric. The analysis then leads to an expression equivalent to (25, 26) but with extra inhomogeneous terms corresponding to the slow variability in the basic state. The compatibility condition will then yield the vKdV equation (1) now with variable coefficients $\mu = \mu(\tau), \delta = \delta(\tau)$, but which are again defined by (31, 32, 33) (but the upper limit in the integrals is now $z = \eta_0$ replacing $z = 0$). For the present case of internal waves, we find that (see the Appendix of Zhou and Grimshaw (1989)

$$Q = c^2 I\,, \quad \nu = -\int_{-h}^{\eta_0} \phi\phi_z F_{0z}\,. \tag{42}$$

Here I is defined by (33)). Note also that the expression for Q can also be simply determined by requiring that QA^2 should be the wave action flux in the linear long wave limit (see, for instance, Grimshaw (1984)).

We shall conclude this section with two illustrative examples. First consider the case of *water waves*. We put the density $\rho =$ constant so that then $N^2 = 0$ (16). Then we obtain the well-known expressions

$$\phi = \frac{z+h}{h} \quad \text{for} \quad -h < z < 0\,, \quad c = (gh)^{1/2}\,. \tag{43}$$

$$\text{and so} \quad \mu = \frac{3c}{2h}\,, \quad \delta = \frac{ch^2}{6}\,, \quad Q = 2gc\,. \tag{44}$$

Similarly, for *interfacial waves*, let the density be a constant ρ_1 in an upper layer of height h_1 and $\rho_2 > \rho_1$ in the lower layer of height $h_2 = h - h_1$. That is

$$\rho_0(z) = \rho_1 H(z + h_1) + \rho_2 H(-z - h_1)\,,$$
$$\text{so that} \quad \rho_0 N^2 = g(\rho_2 - \rho_1)\delta(z + h_1)\,.$$

Here $H(z)$ is the Heaviside function and $\delta(z)$ is the Dirac δ-function. First, let us replace the free boundary with a rigid boundary so that the upper

boundary condition for $\phi(z)$ becomes just $\phi(0) = 0$. This is a good approximation for oceanic internal solitary waves. Then we find that

$$\begin{aligned} \phi &= \frac{z+h}{h_2} \quad \text{for} - h < z < h_1 \,, \\ \phi &= -\frac{z}{h_1} \quad \text{for} - h_1 < z < 0 \,, \\ c^2 &= \frac{g(\rho_2 - \rho_1)h_1 h_2}{\rho_1 h_2 + \rho_1 h_2} \end{aligned} \tag{45}$$

Substitution into (31, (32, 33) yields

$$\begin{aligned} \mu &= \frac{3c(\rho_2 h_1^2 - \rho_1 h_2^2)}{2h_1 h_2(\rho_2 h_1 + \rho_1 h_2)} \,, \\ \delta &= \frac{c h_1 h_2(\rho_2 h_2 + \rho_1 h_1)}{6(\rho_2 h_1 + \rho_1 h_2)} \\ Q &= 2g(\rho_2 - \rho_1)c \,. \end{aligned} \tag{46}$$

Note that for the usual oceanic situation when $\rho_2 - \rho_1 << \rho_2$, the nonlinear coefficient μ for these interfacial waves is negative when $h_1 < h_2$ (that is, the interface is closer to the free surface than the bottom), and is positive in the reverse case. The case when $h_1 \approx h_2$ leads to the necessity to use the extended KdV equation (34).

Next, consider the case when the upper boundary is free, so that

$$\begin{aligned} \phi &= \frac{z+h}{h_2} \quad \text{for} - h < z < h_1 \,, \\ \phi &= \frac{c^2 + gz}{c^2 - gh_1} \quad \text{for} - h_1 < z < 0 \,, \\ \frac{c^4}{g^2} &- \frac{c^2}{g} h + h_1 h_2 \frac{\rho_2 - \rho_1}{\rho_2} = 0 \,. \end{aligned} \tag{47}$$

The expression (47) has two real positive solutions for c^2, namely $c_0^2 > g \max(h_1, h_2) \geq g \min(h_1, h_2) > c_1^2 > 0$, corresponding to the free surface (barotropic) mode and the interface (baroclinic) mode respectively. Substitution into (31, 32, 33) yields

$$I\mu = 3c^2 \Big[\frac{\rho_2}{h_2^2} + \frac{\rho_1 g^3 h_1}{(c^2 - gh_1)^3} \Big] \,,$$

$$
\begin{aligned}
I\delta &= \frac{c^2}{3g}\Big[g\rho_2 h_2 + \frac{\rho_1(c^6-(c^2-gh_1)^3)}{(c^2-gh_1)^2}\Big]\,, \\
I &= 2c\Big[\frac{\rho_2}{h_2} + \frac{\rho_1 g^2 h_1}{(c^2-gh_1)^2}\Big]\,. \qquad (48)
\end{aligned}
$$

It is readily seen that for the free-surface mode, the nonlinear coefficient μ is always positive, but that it can have either sign for the interface mode.

3 Deformation of solitary waves

3.1 Slowly-varying solitary waves: Korteweg-de Vries case

We turn now to the task of obtaining solutions to the vKdV equation (3) when the coefficients $\alpha = \alpha(\tau), \lambda = \lambda(\tau)$. In view of the potential application to internal solitary waves, our focus will be on the effect of variable coefficients on the propagation and deformation of a solitary wave. There are two contrasting limits where asymptotic analysis can be made. In one case the background state changes rapidly from one constant state to another constant state, over a distance much shorter than a typical wavelength. This leads to a disintegration of the solitary wave into several solitary waves, a process often called fissioning. This will be described below in subsection 3.3. In the other case, the background state varies slowly relative to a typical wavelength. In this case the dominant effect is a slow adiabatic deformation of the wave, described as a slowly-varying solitary wave, and discussed in this subsection for the vKdV equation(3) and in the next subsection for the extended vKdV equation (6).

We now suppose that the coefficients α, λ in the vKdV equation are slowly varying, and write

$$
\alpha = \alpha(\sigma)\,, \quad \lambda = \lambda(\sigma)\,, \quad \sigma = \kappa\tau\,, \quad \kappa << 1\,. \qquad (49)
$$

Consistently we also replace ν with $\kappa\nu(\sigma)$. These definitions enable us to define the slowly-varying condition that the half-width (i.e. the width of the wave at the level of one half of the maximum amplitude) should be much less than $1/\kappa$. We then invoke a multi-scale asymptotic expansion of the form (see Johnson (1973a) and Grimshaw (1979))

$$
U = U_0(\psi,\sigma) + \epsilon U_1(\psi,\sigma) + \cdots\,, \qquad (50)
$$

$$\psi = \xi - \frac{1}{\kappa}\int^{\sigma} V(\sigma)\, d\sigma\,. \tag{51}$$

U is defined over the domain $-\infty < \psi < \infty$, and we require that A remain bounded in the limits $\psi \to \pm\infty$. Since we can assume that $\lambda > 0$ small-amplitude waves will propagate in the negative ξ-direction, and so we can suppose that $A \to 0$ as $\psi \to \infty$. However, it will transpire that we cannot impose this boundary condition as $\psi \to -\infty$.

Substitution of (50) into (3) yields,

$$-VU_{0\psi} + \alpha U_0 U_{0\psi} + \lambda U_{0\psi\psi\psi} = 0\,, \tag{52}$$

$$-VU_{1\psi} + \alpha(U_0 U_1)_\psi + \lambda U_{1\psi\psi\psi} = -U_{0\sigma} - \nu U_0\,. \tag{53}$$

Equation (52) has the solitary wave solution

$$U_0 = a\mathrm{sech}^2(K\psi)\,, \tag{54}$$

$$\text{where} \quad V = \frac{\alpha a}{3} = 4\lambda K^2\,. \tag{55}$$

When the coefficients are constants, this is just the well-known KdV solitary wave. Here it is a slowly-varying solitary wave as the amplitude $a = a(\sigma)$, and hence the also the speed $V = V(\sigma), k = k(\sigma)$. The main aim of the analysis is to determine how these parameters vary, and this is determined at the next order of the expansion.

We now seek a solution of (53) for U_1 which is bounded as $\psi \to \pm\infty$, and in fact $U_1 \to 0$ as $\psi \to \infty$. In order to determine the conditions that need to be imposed on the right-hand side of (53) we need to consider the adjoint equation to the homogeneous operator on the left-hand side of (53), which is

$$-VU_{1\psi} + \alpha U_0 U_{1\psi} + \lambda U_{1\psi\psi\psi} = 0\,. \tag{56}$$

Two solutions are $1, U_0$; while both are bounded, only the second solution satisfies the condtion that $U_1 \to 0$ as $\phi \to \infty$. A third solution can be constructed using the variation-of-parameters method, but it is unbounded as $\psi \to \pm\infty$. Hence only one orthogonality condition can be imposed, namely that the right-hand side of (53) is orthogonal to U_0, which leads to

$$\int_{-\infty}^{\infty} U_0(U_{0\sigma} + \nu U_0) d\psi = 0\,. \tag{57}$$

$$\text{or} \quad P_{0\sigma} = 2\nu P_0 \quad \text{where} \quad P_0 = \int_{-\infty}^{\infty} U_0^2\, d\psi\,. \tag{58}$$

As the solitary wave (54) has just one free parameter (e.g. the amplitude a), this equation suffices to determine its variation. Substituting (54, 55) into (58) yields

$$P_0 = \frac{4a^2}{3K}\,, \tag{59}$$

$$\text{and so} \quad a^3 = C\frac{\alpha}{\lambda}\exp\left(-4\int^{\sigma}\nu d\sigma\right), \tag{60}$$

where C is a constant of integration. Note that in the conservative case when $\nu = 0$, this expression (60) is a simple algebraic expression for the variation of the amplitude.

We now recall that the vKdV equation possesses two conservation laws

$$\frac{\partial M}{\partial \tau} = -\nu M\,, \quad M = \int_{-\infty}^{\infty} U dx\ , \tag{61}$$

$$\frac{\partial P}{\partial \tau} = -2\nu P\,, \quad P = \int_{-\infty}^{\infty} U^2 dx\,, \tag{62}$$

for mass and momentum respectively, and express the conservation of M, P in the conservative case when $\nu = 0$. The condition (57) is easily recognized as the leading order expression for conservation of momentum (62). But since this completely defines the slowly-varying solitary wave, we now see that this cannot simultaneously conserve total mass. This is also apparent when one examines the solution of (53) for U_1, from which it is readily shown that although $U_1 \to 0$ as $\psi \to \infty$, $A_1 \to D_1$ as $\psi \to -\infty$ where

$$VD_1 = -M_{0\sigma} - \nu M_0\,, \tag{63}$$

$$\text{where} \quad M_0 = \int_{\infty}^{\infty} U_0 d\psi = \frac{2a}{K}\,. \tag{64}$$

This non-uniformity in the slowly-varying solitary wave has been recognized for some time, see, for instance, Grimshaw and Mitsudera (1993) and the references therein. The remedy is the construction of a trailing shelf U_s of small amplitude $O(\kappa)$ but long length-scale $O(1/\kappa)$, which thus has $O(1)$ mass, but $O(\kappa)$ momentum. It resides behind the solitary wave, and to leading order is given by

$$U_s = \kappa U_s(\Xi)\exp\left(-\int_{\Sigma}^{\sigma}\nu d\sigma\right), \quad \Xi = \kappa\xi < \Psi(\sigma) = \int^{\sigma} V d\sigma\,. \tag{65}$$

Here $\Xi = \Psi(\sigma)$ defines the location of the solitary wave, and $\Sigma(\Xi)$ is the inverse of this defining relation, that is, $\Xi = \Psi(\Sigma(\Xi))$ is an identity in Ξ. $U_s(\Xi)$ is independent of σ, and is determined so that the shelf amplitude is just $\kappa D_1(\sigma)$ at the location of the solitary wave, that is $U_s(\Phi(\sigma)) = D_1$ (63). At higher orders in κ the shelf itself will evolve and may generate secondary solitary waves (El and Grimshaw (2002) and Grimshaw and Pudjaprasetya (2004)). It may readily be verified that the slowly-varying solitary wave and the trailing shelf together satisfy conservation of mass.

In the conservative case when $\nu = 0$ the expressions (60) and (63) reduce to

$$a^3 = C\frac{\alpha}{\lambda}\,, \quad D_1 = \frac{a_\sigma}{2\lambda K^3} \tag{66}$$

These expressions show that the amplitude increases (decreases) as α/λ increases (decreases), and that the trailing shelf then has the same (opposite) polarity (recall that the sign of α determines the polarity of the solitary wave). A particular case of interest is when the nonlinear coefficient α passes through zero, while λ stays finite. The prediction from the adiabatic formula (71) is that the solitary wave amplitude goes to zero, and so the solitary is destroyed. The outcome of this situation needs numerical simulations, and these will be described below in section 4.

3.2 Slowly-varying solitary waves: extended Korteweg-de Vries case

We now turn to the variable-coefficient extended KdV equation (6), where we can use the same multi-scale asymptotic expansion used in subsection 3.1, that is, (49, 50) with (51). The leading term is the solitary wave now given by

$$U_0 = \frac{D}{1 + B\cosh K\psi}\,, \tag{67}$$

$$\text{where} \quad V = \frac{\alpha D}{6} = \lambda K^2\,, \tag{68}$$

$$\text{and} \quad B^2 = 1 + \frac{6\lambda\beta K^2}{\alpha^2}\,. \tag{69}$$

The amplitude is $a = D/1 + B$. The family of solutions (67) depend on a single parameter, which can conveniently be taken as B, and are displayed in Figure 3. As before, we take $\lambda > 0$ without loss of generality. Then, for $\beta < 0$

there is just one branch of solutions, with $0 < B < 1$; they range from small-amplitude solitary waves of KdV-type with the familiar "sech^2"-profile when $B \to 1$, to a limiting wave of amplitude $-\alpha/\beta$ as $B \to 0$; this limiting wave is characterized by a flat top, and are sometimes called "table-top" waves. For $\beta > 0$ there are two branches; one has $1 < B < \infty$ and ranges from small-amplitude KdV-type waves when $B \to 1$, to arbitrarily large waves with a "sech"-profile as $B \to \infty$. The other branch has has the opposite polarity, exists for $-\infty < B < -1$, and ranges from arbitrarily large waves with a "sech"-profile to a limiting algebraic solitary wave of amplitude $-2\alpha/\beta$. Solitary waves with smaller momentum cannot exist, and from the point of view of the associated spectral problem are replaced by breathers, that is, pulsating solitary waves (see, for instance, Clarke et al 2000, Grimshaw et al 1999, Pelinovsky and Grimshaw 1997).

We now follow the same procedure described in subsection 3.1. That is, the determination of how the key parameter B of (67) varies with σ is found either by considering the next-order term in the expansion, or equivalently by using the conservation law (62) for momentum, which can easily be shown to also hold for the variable-coefficient extended KdV equation (6). The outcome is that (57) holds for the solitary wave (67) and so we get that

$$P_0 = \frac{D^2}{K}\int_{-\infty}^{\infty} \frac{du}{(1+B\cosh u)^2} = C\exp\left(-2\int^{\sigma}\nu d\sigma\right), \tag{70}$$

$$\text{or} \quad G(B) = C\left|\frac{\beta^3}{\lambda\alpha^2}\right|^{1/2}\exp\left(-2\int^{\sigma}\nu d\sigma\right), \tag{71}$$

$$\text{where} \quad G(B) = |B^2-1|^{3/2}\int_{-\infty}^{\infty}\frac{du}{(1+B\cosh u)^2}\,. \tag{72}$$

Here C is again a constant of integration. The integral term in $G(B)$ can be explicitly evaluated, and so we finally get

$$B^2 > 1: \quad G(B) = 2(B^2-1)^{1/2} \mp 4\text{arctan}\sqrt{\frac{B-1}{B+1}}\,, \tag{73}$$

$$0 < B < 1: \quad G(B) = 4\text{arctanh}\sqrt{\frac{1-B}{1+B}} - 2(1-B^2)^{1/2}\,. \tag{74}$$

The alternative signs in (73) correspond to the cases $B > 1$ or $B < -1$. Expressions of this type have been used by Egorov (1993) for water waves, and Grimshaw et al (1999, 2004) for internal waves.

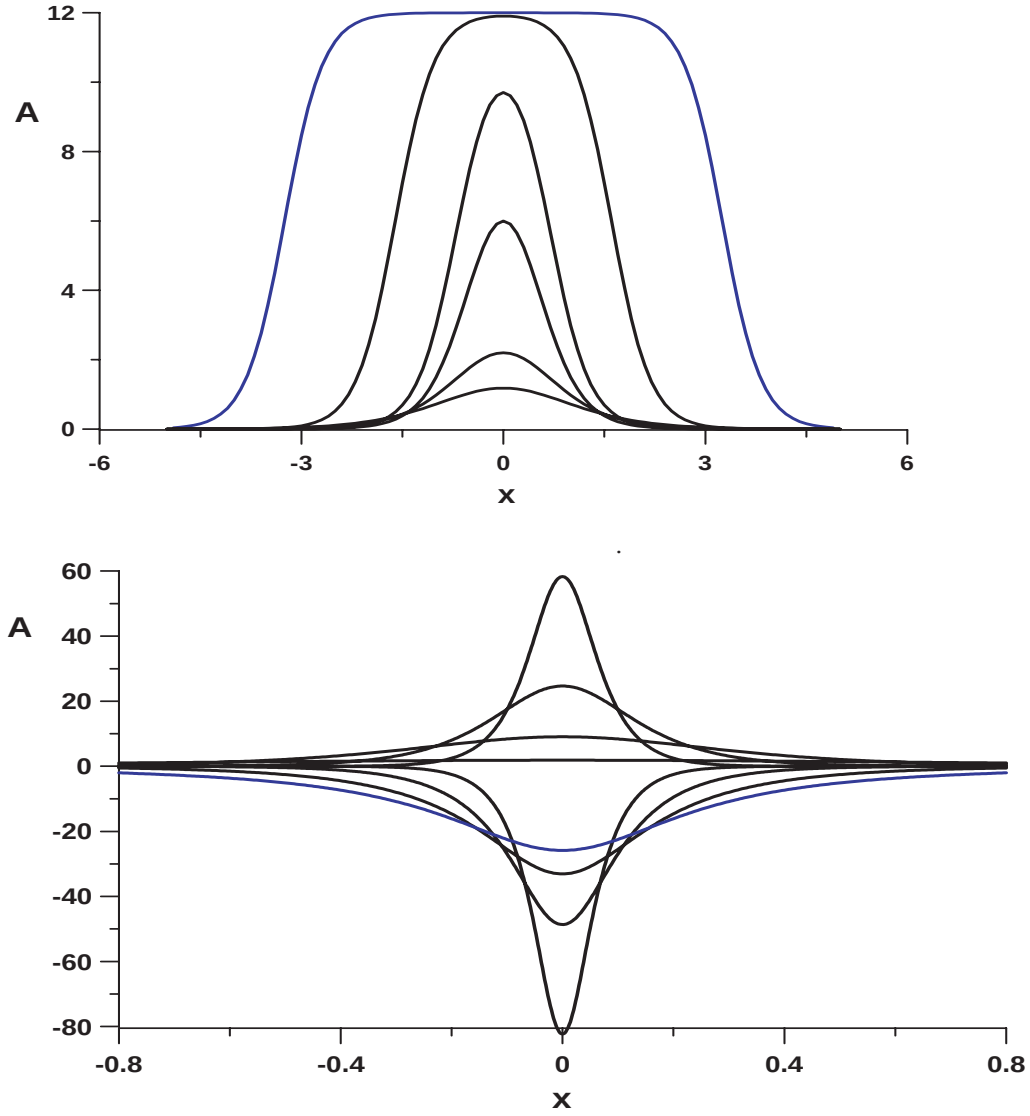

Figure 2: The solitary wave family (67). The upper panel is for $\beta < 0$ and the lower panel is for $\beta > 0$; in both panels $\alpha > 0, \lambda > 0$.

Next, just as for the vKdV case discussed in subsection 3.1, the slowly-varying solitary wave is accompanied by a trailing shelf, in order to conserve total mass. To leading order it is determined exactly as described in subsection 3.1, and so is given by (65) where here

$$B^2 > 1 : \quad M_0 = \pm|\frac{6\lambda}{\beta}|^{1/2}\, 4\mathrm{arctan}\sqrt{\frac{B-1}{B+1}}\,, \tag{75}$$

$$0 < B < 1 : \quad M_0 = \pm|\frac{6\lambda}{\beta}|^{1/2}\, 4\mathrm{arctanh}\sqrt{\frac{1-B}{1+B}}\,. \tag{76}$$

Here the alternative signs in (75) and (76) correspond to the cases $\alpha B > 0$ or $\alpha B < 0$.

The expression (71) provides an explicit formula for the dependence of B on the environmental parameters $\alpha, \beta, \lambda, \nu$. It is readily shown that $G(B)$ (73) is a monotonically increasing function of $|B|$ for $1 < |B| < \infty$, and is a monotonically decreasing function of B for $0 < B < 1$ (74). For the conservative case when $\nu = 0$, we see that as $|\beta^3/\lambda\alpha^2| \to \infty$, then so does $G(B)$; we infer that then, if $\beta < 0$ so that $0 < B < 1$, $B \to 0$ and the wave approaches the limiting "table-top" shape. On the other hand if $\beta > 0$ and $1 < |B| < \infty$ then $|B| \to \infty$ and the wave shape approaches the "sech"-profile, The behaviour of the wave amplitude in these limits depends on the behaviour of each of the parameters α, β, λ. But since we can usually expect $\lambda(> 0)$ to be finite and bounded away from zero, we see that these limiting shapes are achieved only as either $\beta \to \infty$, or as $\alpha \to 0$. For the case when $\beta \to \infty$, with α, λ remaining finite and bounded away from zero, it is readily shown from (71, 73) that $|B| \sim \beta^{3/2}$, and then (68, 69) show that the amplitude behaves as $a \sim \beta^{1/2}$ and $K \sim \beta$. On the other hand, when $\beta \to -\infty$, again with α, λ remaining finite and bounded away from zero, it is readily shown from (72, 74) that $G(B) \sim \beta^{3/2}$ and $B \sim 2\exp(-G/2)$, and then (68, 69) show that the amplitude behaves as $a \sim -\alpha/\beta$ and $K \sim 1/\beta^{1/2}$. This is the limiting "table-top" wave, of increasing width. We note here that as the width of the "table-top" wave increases, the basic assumption that the wave width is much less than the scale of the background variability (expressed through the variable coefficients) will be violated, leading to an eventual breakdown of the adiabatic behaviour. The case when $\alpha \to 0$ is more complicated, and will be described below in section 4.

On the other hand, again with $\nu = 0$, we see that as $|\beta^3/\lambda\alpha^2| \to 0$, then so does $G(B)$. In this case $B \to 1$, $G(B) \sim |B-1|^{3/2}$ (see (73, 74)) and the

wave profile reduces to the KdV "sech^2"-shape, provided that either $\beta < 0$ when $0 < B < 1$, or if $\beta > 0$, then the wave initially belongs to the branch defined by $1 < B < \infty$. But if $\beta > 0$ and the wave initially belongs to the branch defined by $-\infty < B < -1$, then the limit $G(B) \to 0$ cannot be achieved; instead we expect a transition to a breather. Let us suppose that this limiting situation is achieved by $|\alpha| \to \infty$, with $|\beta|, \lambda$ remaining bounded. Then it follows from (71, 74) that $|B-1| \sim 1/|\alpha|^{2/3}$, and then (68, 69) show that $K \sim |\alpha|^{2/3}$ and the amplitude behaves as $a \sim |\alpha|^{1//3}$, in agreement with the vKdV result (66). The alternative case when $|\beta| \to 0$ is more complicated and will be described below in section 4.

3.3 Fission

Here we suppose that the background state changes rapidly from one constant state to another constant state, over a distance much shorter than a typical wavelength. Consider the conservative case when $\nu = 0$, and suppose that is, in the vKdV equation (3) (and in the evKdV equation (6)), the coefficients $\alpha(\tau), \lambda(\tau)$ (and $\beta(\tau)$) vary rapidly with respect to the wavelength of a solitary wave. Suppose, for instance that the coefficients make a rapid transition from the values $\alpha_-, \lambda_-\, (\beta_-)$ in $\tau < 0$ to the values $\nu_+, \lambda_+, (\beta_+)$ in $\tau > 0$. Then a steady solitary wave can propagate in the region $\xi < 0$, given in the vKdV case by (see (54. 55))

$$U \;=\; a\,\mathrm{sech}^2(K(\xi - V\tau))\,, \quad V = \frac{\alpha_- a}{3} = 4\lambda_- K^2\,. \tag{77}$$

For the evKdV equation, the corresponding expression is (see (67, 68, 69))

$$U = \frac{D}{1 + B\cosh K(\xi - V\tau)}\,, \quad V = \frac{\alpha D}{6} = \lambda K^2\,, \quad B^2 = 1 + \frac{6\lambda\beta K^2}{\alpha^2}\,. \tag{78}$$

It will pass through the transition zone $\tau \approx 0$ essentially without change. However, on arrival into the region $\tau > 0$ it is no longer a permissible solution of (3), which now has constant coefficients ν_+, λ_+ (and β_+). Instead, with $\tau = 0$, the expression (77) (and (78)) now forms an effective initial condition for the new constant-coefficient KdV (and eKdV) equation. Both the KdV and the eKdV are integrable equations, and the theory based on the inverse scattering transform can be used to predict the outcome. In general, this initial condition will evolve into a number of *solitons*, and it is this process which is called *fission*. Numerical simulations of the vKdV and eKdV

equations for the stated conditions on the coefficients, that is a rapid transfer form one set of constant values to another set, confirm this general scenario.

In the case of the KdV equation, an explicit expression can be derived for the amplitude of these solitons (see Tappert and Zabusky (1971), Johnson (1972) for an application to water waves, Djordevic and Redekopp (1978) for an application to internal waves and Zheng et al (2001) for an application to observations of fissioning of internal solitary waves in the Gulf of Aden). The KdV equation is exactly integrable using an associated spectral problem, with the inverse scattering transform, from which the solution in $\tau > 0$ can now be constructed. Indeed in this case the spectral problem has an explicit solution (e.g. Drazin and Johnson, 1989). The outcome is that the initial solitary wave fissions into N solitons, and some radiation. The number N of solitons produced is determined by the ratio of coefficients $R = \alpha_+\lambda_-/\alpha_-\lambda_+$. If $R > 0$ (i.e. there is no change in polarity), then $N = 1+[((8R+1)^{1/2}-1)/2]$ ($[\cdots]$ denotes the integral part); as R increases from 0, a new soliton (initially of zero amplitude) is produced as R successively passes through the values $m(m+1)/2$ for $m = 1, 2, \cdots$. But if $R < 0$ (that is, there is a change in polarity) no solitons are produced and the solitary wave decays into radiation.

4 Passage through critical points

The analysis of the adiabatic transformation of a solitary wave in subsections 3.1 and 3.2 shows that the critical points where $\alpha = 0$, or where $\beta = 0$ are sites where we may possibly expect a dramatic change in the wave structure. We consider only the conservative case when $\nu = 0$ and at first examine the vKdV model (3) so that $\beta = 0$. Let us then suppose that $\alpha = 0$ at $\sigma = 0$, where, without loss of generality, we can assume that α passes from negative to positive values as σ increases. Initially the solitary wave is located in $\sigma < 0$ and has negative polarity. Then, near the transition point, the amplitude of the wave decreases to zero as $a \sim -|\alpha|^{1/3}$, while $K \sim |\alpha^{2/3}|$; the momentum of the solitary wave is of course conserved (at least to leading order), the mass of the solitary wave increases (in absolute value) as $1/|\alpha^{1/3}|$, its speed decreases as $\alpha^{4/3}$, and the amplitude D_1 of the trailing shelf just behind the solitary wave grows as $1/|\alpha|^{8/3}$; the total mass of the trailing shelf grows as $1/|\alpha|^{1/3}$, in balance with that of the solitary wave, while the total mass remains a negative constant. Since the tail grows to be comparable with the wave itself, the adiabatic approximation breaks down as the critical

point is approached. Nevertheless, we can infer that the the solitary wave itself is destroyed as the wave attempts to pass through the critical point $\alpha = 0$. The structure of the solution beyond this critical point has been examined numerically by Grimshaw et al (1998a), who showed that the shelf passes through the critical point as a positive disturbance, which then being in an environment with $\alpha > 0$, can generate a train of solitary waves of positive polarity, riding on a negative pedestal (see Figure 2). Of course, these conclusions may need to be modified when the cubic nonlinear term in (6) is taken into account near the critical point (Grimshaw et al, 1999), and this issue is taken up later in this section.

In a typical oceanic situation, where there is a relatively sharp near-surface pycnocline, an internal solitary wave of depression is generated in the deep water and propagates shorewards until it reaches a critical point. For a simple two-layer model, this is where the pycnocline is close to the mid-depth (see 46). The theory described above then predicts that this wave will be destroyed in the vicinity of this critical point and replaced in the shallow water shorewards of the critical point by one or more internal solitary waves of elevation riding on a negative pedestal. This basic scenario has been observed in several places in the ocean, For instance, this phenomena has been reported by Salusti et al (1989) in the Eastern Mediterranean, by Holloway et al (1997, 1999) in the North West Shelf of Australia, by Hsu et al (2000) in the East China Sea, and recently during the ASIEX experiment in the South China Sea by Duda et al (2004), Liu et al (2004), Orr and Mignerey (2003), Ramp et al (2004), Yang et al (2004), and Zheng et al (2003). But elsewhere in the ocean, where there are no such critical points, the shoreward propagating small-amplitude internal solitary waves are expected to deform adiabatically (at least within the framework of the vKdV equation). Examples of this behaviour occur on the Malin Shelf off the North-west coast of Scotland, see Small (2003), Grimshaw et al (2004) and Small and Hornby (2005), and in the Laptev Sea in the Arctic, see Grimshaw et al (2004).

We next take account of the cubic nonlinear term in (6) and so suppose that α passes through zero (again with $\nu = 0$), but that $\beta \neq 0$ at the critical point $\sigma = 0$ where $\alpha = 0$. First, let us suppose that $\beta < 0, 0 < B < 1$. Then as $\alpha \to 0$, we see from (71) and (74) that $G(B) \sim 1/|\alpha|$, and $B \to 0$ with $B \sim 2\exp(-G/2)$. Thus the approach to the limiting "table-top" wave is quite rapid. From (68. 69) we see that in this limit, $K \sim |\alpha|$ and the amplitude approaches the limiting value $a \sim -\alpha/\beta$. Thus the wave amplitude decreases to zero, and, interestingly, this is a more rapid destruction of the solitary

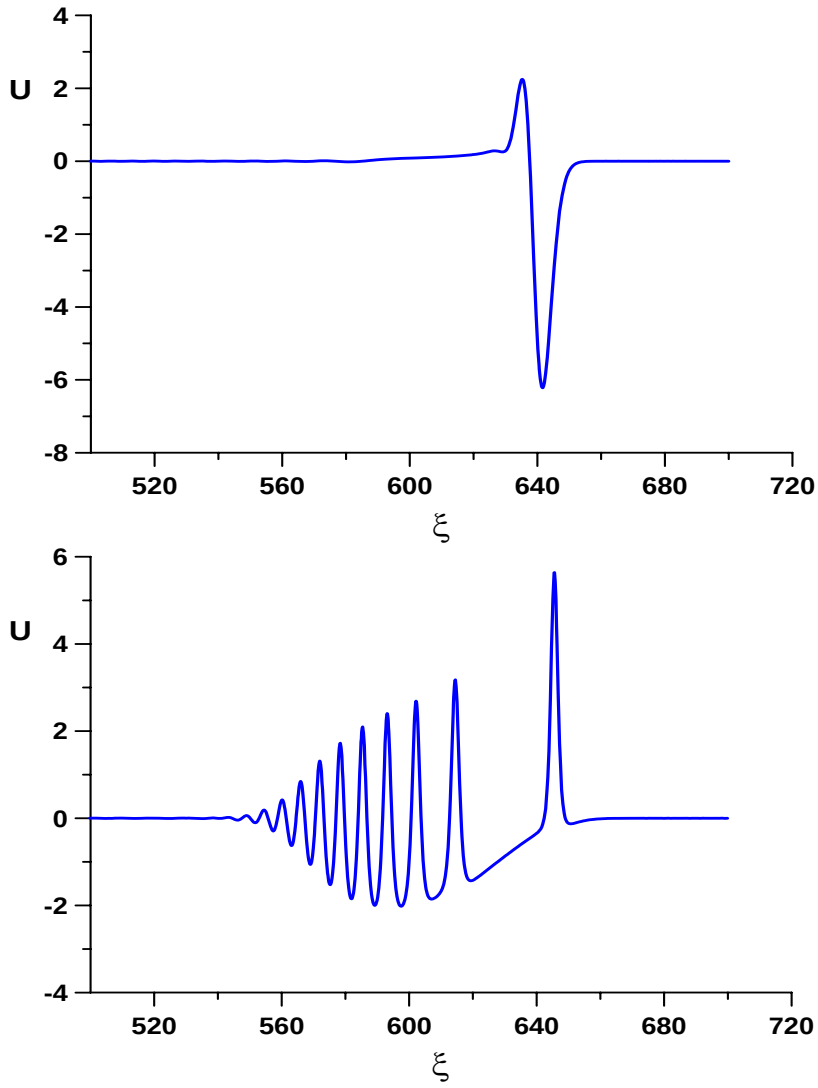

Figure 3: A numerical simulation of the vKdV equation (3) for the case when $\delta = 1, \nu = 0$ and α varies from -1 to $+1$. The upper panel is when $\alpha = 0$ and the lower panel is when $\alpha = +1$. The simulation shows a strong deformation of the initial solitary wave of depression at $\alpha = 0$, followed at $\alpha = 1$ by the emergence of a number of solitary waves of elevation.

wave than for the case when $\beta = 0$. The mass M_0 (76) of the solitary wave grows as $|\alpha|^{-1}$ and so the amplitude D_1 of the trailing shelf (63) grows as $1/|\alpha|^4$. The overall scenario after α has passed through zero is similar to that described above for the vKdV equation (3) and has been discussed in detail by Grimshaw et al (1999). Essentially the trailing shelf passes through the critical point as a disturbance of the opposite polarity to that of the original solitary wave, which then being in an environment with the opposite sign of α, can generate a train of solitary waves of the opposite polarity, riding on a pedestal (see Figure 4 for an example where a "table-top" solitary wave is converted to another such wave of opposite polarity, riding on a pedestal).

Next, let us suppose that $\beta > 0$ so that $1 < |B| < \infty$ There are the two sub-cases to consider, $B > 0$ or $B < 0$, when the the solitary wave has the same or opposite polarity to α. Then, as $\alpha \to 0, |B| \to \infty$ as $|B| \sim 1/|\alpha|$. It follows from (68. 69) that then $K \sim 1$, $D \sim 1/|\alpha|, a \sim 1, M_0 \sim 1$. It follows that the wave adopts the "sech"-profile, but has *finite* amplitude, and so can pass through the critical point $\alpha = 0$ without destruction. But the wave changes branches from $B > 0$ to $B < 0$ as $|B| \to \infty$, or *vice versa*. An interesting situation then arises when the wave belongs to the branch with $-\infty < B < -1$ and the amplitude is reducing. If the limiting amplitude of $-2\alpha/\beta$ is reached, then there can be no further reduction in amplitude for a solitary wave. Instead a breather will form. An example of this outcome is shown in Figure 5, where the wave has entered this regime after passing through the critical point. Of course, such a transformation to a breather can occur without the necessity to pass through a critical point. For instance, the wave amplitude could be reduced by the action of friction, and an instance of breather formation by this process is described by Grimshaw etal (2003).

Finally, we consider the situation when $\beta \to 0$, $\alpha \neq 0$ but again $\nu = 0$. This case has been studied by Nakoulima et al (2004) using both an asymptotic analysis analogous to that used here, and direct numerical simulations. As already noted above, in this case $B \to 1$, $G(B) \sim |B-1|^{3/2}$ (73, 74), and it then follows from (71) that $G \sim |\beta|^{3/2}$ and so $|B-1| \sim |\beta|$. There are three sub-cases to consider. First, suppose that initially $\beta < 0$ and so $0 < B < 1$. As $|\beta| \to 0$, $1 - B \sim |\beta|$ and the wave profile becomes the familiar KdV "sech^2"-shape. It is readily shown from (68, 69) that then $K, a, M_0, D_1 \sim 1$ and so the wave can pass through the critical point $\beta = 0$ without destruction. However, after passage through the critical point, the wave has moved to a different solitary branch (see Figure 3), and this may change its ultimate fate. A typical scenario is shown in Figure 6, which shows

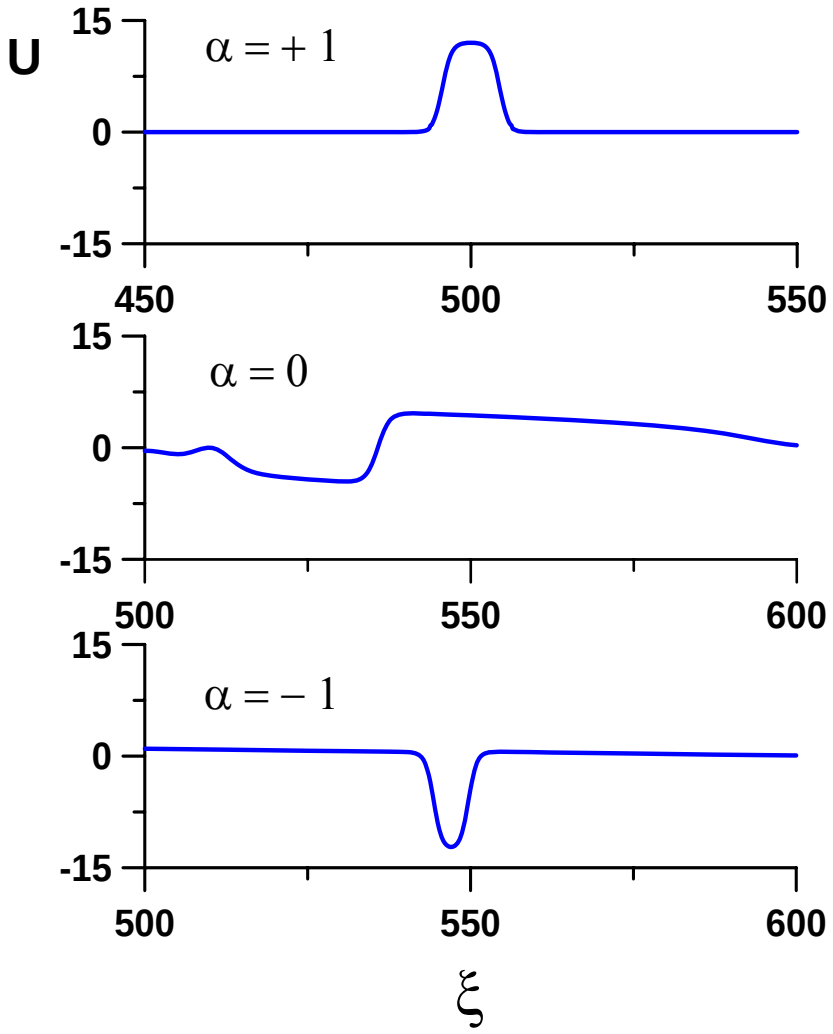

Figure 4: A numerical simulation of the evKdV equation (6) for the case when $\delta = 1, \beta = -0.083, \nu = 0$ and α varies from 1 to -1. The upper panel shows the initial condition of a "table-top" solitary wave of elevation at $\alpha = -1$, the middle panel shows a strong deformation at $\alpha = 0$, and the lower panel shows the leading wave at $\alpha = +1$. This wave is another "table-top" wave, but now one of depression riding on a small positive pedestal

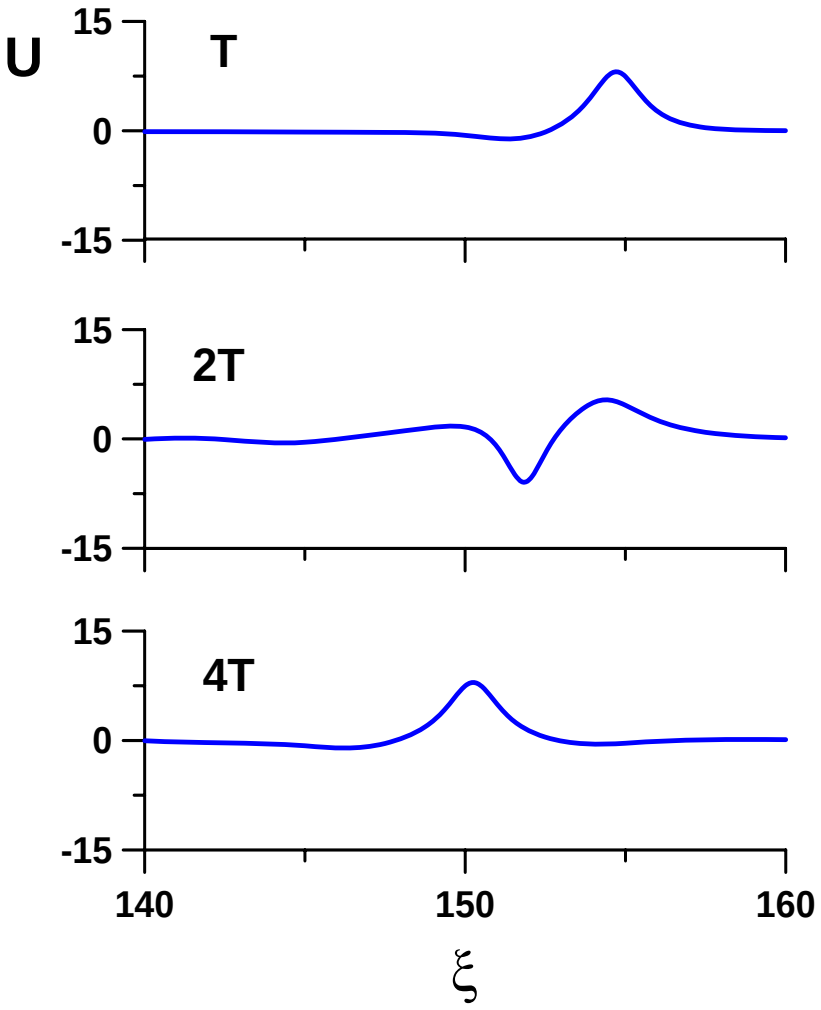

Figure 5: A numerical simulation of the evKdV equation (6) for the case when $\delta = 1, \beta = 0.3, \nu = 0$ and α varies from 1 to -1. The initial wave (not shown) is a solitary wave of elevation belonging to the branch for which $B > 0$. It then passes adiabatically through the critical point , changing the sign of B to $B < 0$, and arrives at the location $\alpha = -1$ at a time $\tau = T$ with only a small deformation. However, at this stage its amplitude is below that allowed for a steady solitary wave, and so it deforms into a breather, shown in the middle panel for $\tau = 2T$ and the lower panel for $\tau = 4T$

the transformation of a "table-top" solitary wave (upper panel in Figure 3) to a KdV "sech^2"-KdV solitary wave at the critical point, and further evolution as a solitary wave of the upper branch in the lower panel of Figure 3. Second, suppose that initially $\beta > 0$ and $1 < B < \infty$. Now $B - 1 \sim \beta$ and again the wave profile becomes the familiar KdV "sech^2"-shape, while $K, a, M_0, D_1 \sim 1$, allowing the wave to pass through the critical point $\beta = 0$ without destruction, but moving now form the upper branch in the lower panel of Figure 3 to the "table-top" brach in the upper panel of Figure 3. Third, suppose that initially $\beta > 0$ and $-1 > B > -\infty$. In this case it an be shown from (73) that $G(B)$ decreases from ∞ to a finite value of 2π as B increases from $-\infty$ to -1. Consequently the limit $\beta \to 0$ in (71) cannot be achieved. Instead as β decreases the limit $B = -1$ is reached, when the wave has become an algebraic solitary wave. Presumably a further decrease in β would generate breathers.

5 Oceanic applications and discussion

As we have already mentioned in Section 1 and elsewhere, the vKdV and the extended vKdV equations (3) (or (1)) and (6) (or (5)) have been extensively used to model the evolution of internal solitary waves over topography in the coastal oceans. For instance, Grimshaw et al (2004) used the extended vKdV equation (6) to study the deformation of an internal solitary wave as it evolves over three representative continental shelves, the North West Shelf (NWS) of Australia, the Malin Shelf off the North West coast of Scotland, and the Laptev Sea in the Arctic. In Figure 7 we display the coefficients of the extended vKdV equation (5) (note the relations (4, 7) between these coefficients and those of (6)) for the NWS, using data from the section from the point $(19.2^oS, 115.7^oE)$ to the point $(19.8^oS, 116.5^oE)$ along which CTD data were obtained in January 1995 (see Holloway et al (1997,1999)). Only the topography and the density stratification were used to evaluate these coefficients, and any effect of background currents was ignored, so that $\nu = 0$ here. We see that as the depth decreases the linear magnification factor Q, the linear phase speed c and the linear dispersive coefficient δ all decrease; this is to be expected, as in general they can be expected to scale approximately as $h^{1/2}, h^{1/2}$ and $h^{5/2}$ respectively. In particular, the dramatic decrease in δ can be expected to enhance the effect of nonlinearity as the wave propagates shoreward (see the adiabatic expression (66) for instance). From Figure 7

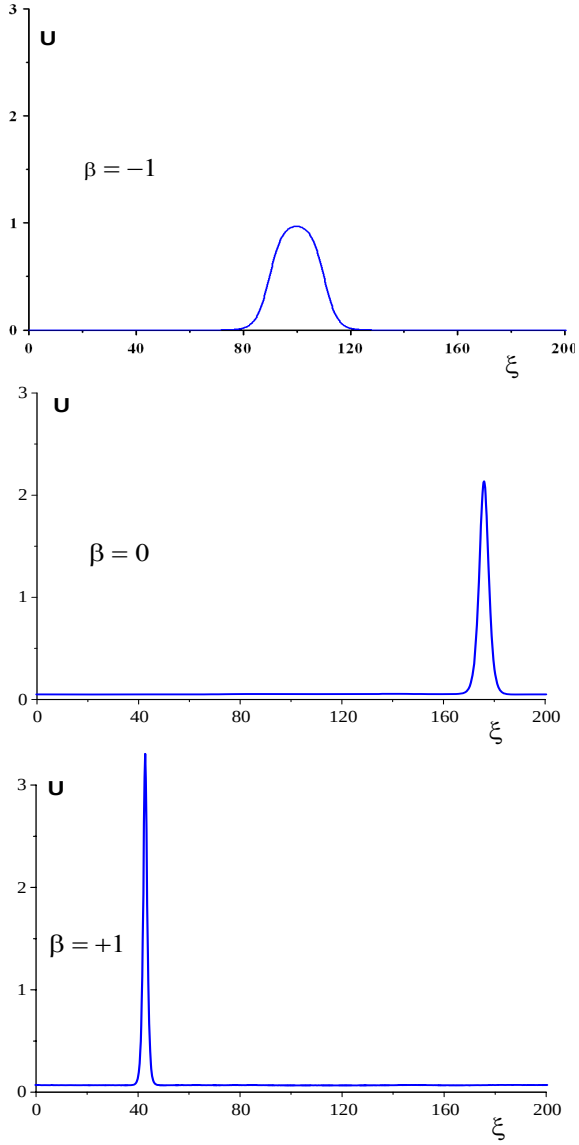

Figure 6: A numerical simulation of the evKdV equation (6) with $\alpha = 1, \lambda = 1, \nu = 0$ and β varies from -1 to 1, showing the transformation of a "table-top" solitary wave to a KdV "sech^2"-KdV solitary wave at the critical point, and further evolution as a solitary wave tending to a "sech"-profile.

we see that there are three critical points where the quadratic coefficient $\mu = 0$ at approximately $45, 59, 61km$ and μ is almost zero again at $93km$; the cubic coefficient μ_1 is initially quite small and vanishes at approximately $13, 31, 41km$ and again at $68km$. Consequently, we expect the internal solitary wave to evolve adiabatically as a wave of depression up to about $45km$ along the path, after which it will deform according to the critical point scenarios described above.

In Figure 8, we display the evolution along the NWS of an internal solitary wave whose initial amplitude is $10m$ (see Grimshaw et al (2004) for analogous results for initial amplitudes of $5, 15m$). As expected, the evolution is adiabatic up to $45km$. At this critical point $\mu_1 > 0$ and so the wave can pass through this critical point without destruction. But then, for a relatively short distance (from 42 to $48km$) the cubic coefficient μ_1 grows by a factor of 10, inducing a large amplification in the wave amplitude (a factor of 2). The tail behind the solitary wave forms mainly at this stage. Between the next set of critical points at $59, 61km$ where $\mu = 0$ but $\mu_1 > 0$, we see that the the leading wave can again avoid complete desruction, but the tail has grown substantially and has formed a negative pulse behind the main wave. Then, after passage through the critical point at $68km$ where the cubic coefficient μ_1 changes sign from positive to negative, both negative solitary-like waves disappear forming dispersive wave packets; this is to be expected as when $\mu > 0, \mu_1 < 0$ only positive solitary waves are allowed (see the upper panel of Figure 2) and so the negative pulses must disperse. But because here the dispersive waves are energetic enough, a group of solitary waves of positive polarity is ultimately generated, and are visible at $85km$.

The simulation shown in Figure 8, together with many other similar simulations and observations demonstrate the key role played by the coefficients of the extended vkdv equation (5). Hence, in Figure 9, we display world maps of these coefficients, based on the long-term mean annual hydrologic data with one-degree latitude-longitude resolution given by Levitus and Boyer (1994). As expected, the linear phase speed c and the linear dispersive coefficient scale approximately with $h^{1/2}$ and $h^{5/2}$ respectively, and hence, as is well-known, the largest amplitude internal solitary waves will generally be found in the shallow seas of the coastal zones. However, the quadratic and cubic coefficients μ and μ_1 show considerable variability, with many sign changes, thus emphasising again the importance of critical points. Analogous maps for specific regions of interest have been developed by Ivanov et al (1994) for the Black Sea, by Pelinovsky et al (1995) for the coast of Israel, by Talipova

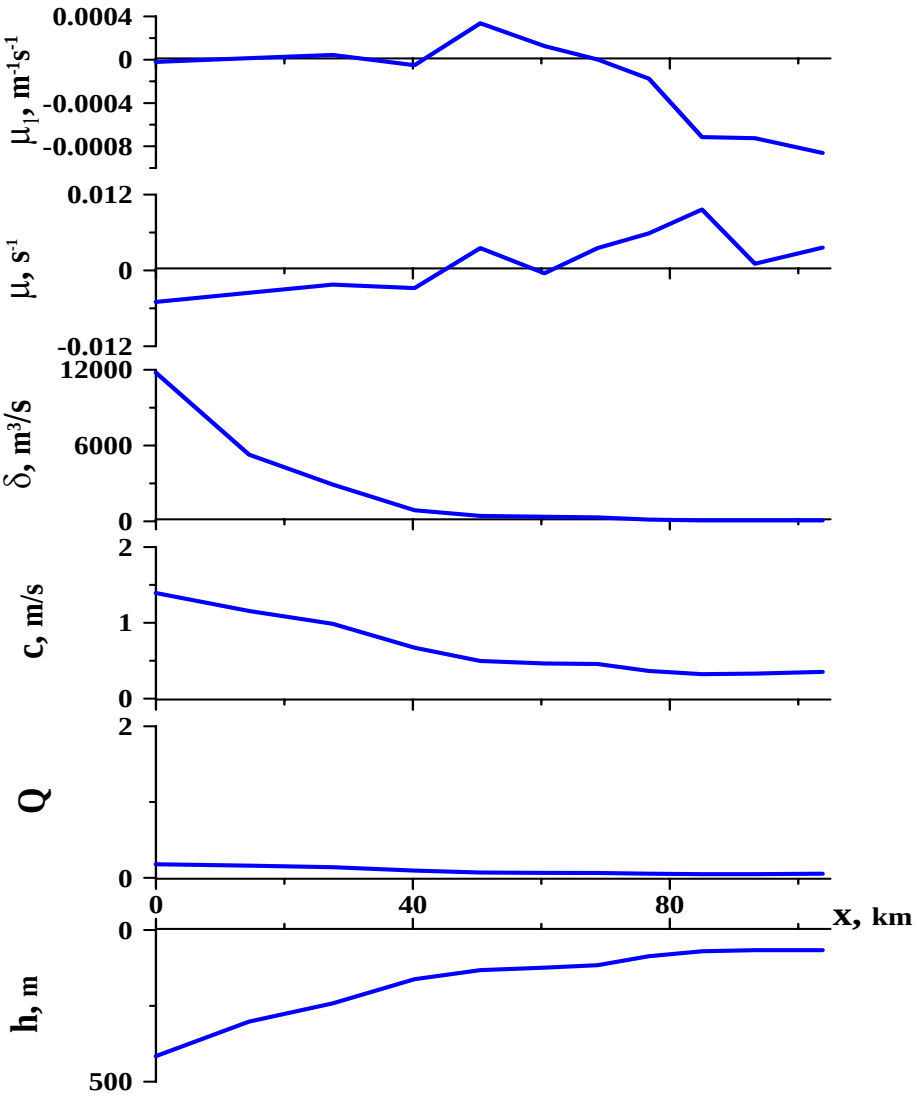

Figure 7: Coefficients of the extended vKdV equation (5) for the North West Shelf (NWS) of Australia, plotted as distance across the shelf from the initial point at a depth of $416m$.

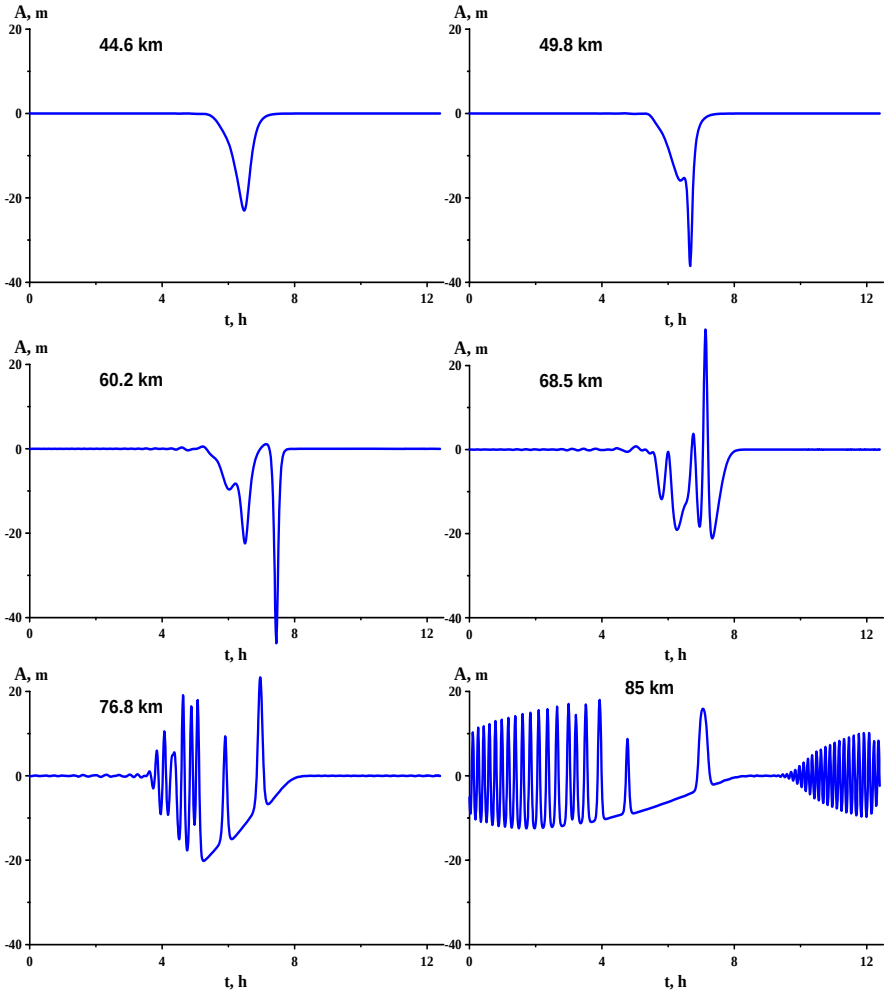

Figure 8: Transformation of a solitary wave with initial amplitude $10m$ across the NWS. The plots show the time evolution at the indicated locations. The oscillations at the right-hand side of the plot at $85km$ are a consequence of the periodic conditions used in the simulations.

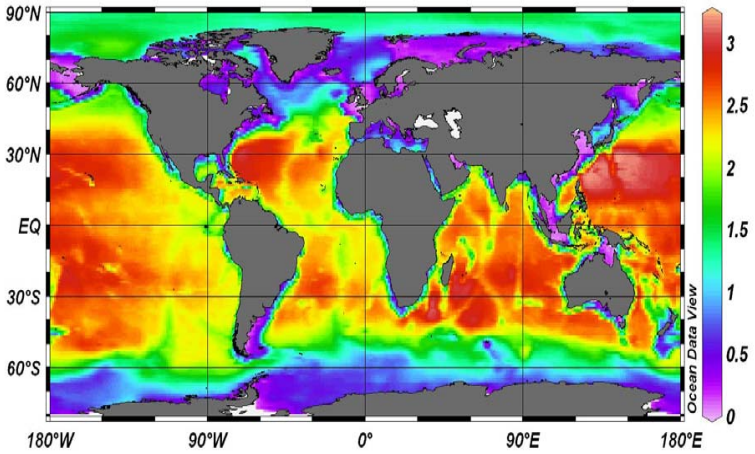

a) speed of propagation, c (m/s)

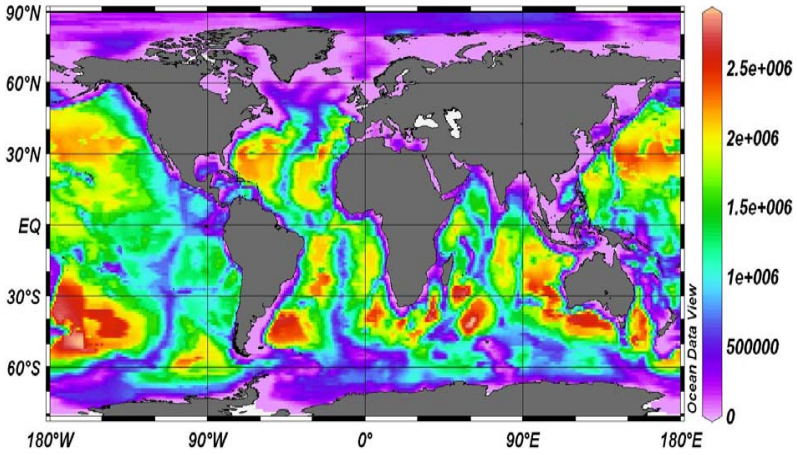

b) dispersion coefficient, δ (m^3/s)

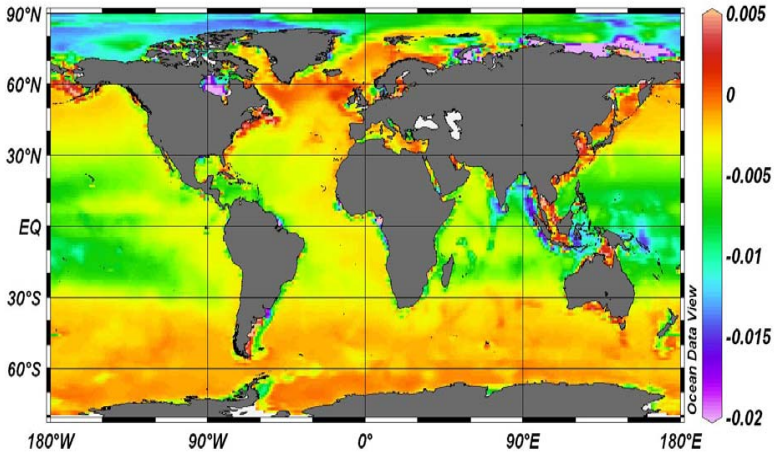

c) coefficient of quadratic nonlinearity, μ (s^{-1})

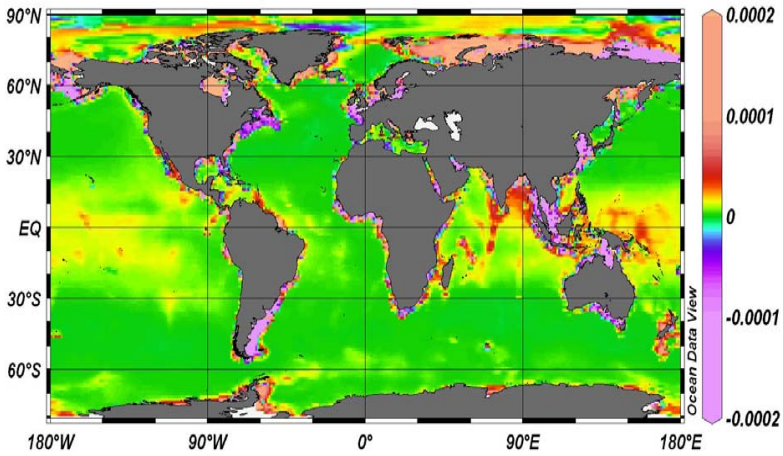

d) coefficient of cubic nonlinearity, μ_1 ($m^{-1}s^{-1}$)

Figure 9: World maps of the coefficients of the extended vKdV equation (5)

et al (1998) for the Baltic Sea, and by Poloukhin et al (2003, 2004) for the Arctic Sea (the last paper also took account of background currents).

Our focus in this survey article has been on modeling the deformation of oceanic internal solitary waves as they propagate through a variable medium, such as that provided by the topography of the continental shelf and the changing hydrography from deep to shallow water. For this purpose we have used the variable-coefficient extended Korteweg-de Vries equation (6), since on the one hand it is a valid and much-used model in this context, and on the other hand it allows for a quite detailed analysis. However, we should mention that there have been many numerical simulations of internal solitary waves, using a variety of other model systems, ranging from Boussinesq-type equations to the full Euler equations. But, relatively few of these simulations have focussed directly on the issue of how an internal solitary wave deforms over the continental shelf. More often they examine the generation process due to the interaction of a current with topography, together with the propagation over topography, and hence cannot easily identify the deformation processes alone. Nevertheless, it is pertinent to note here the simulations of the full Euler equations by Lamb (2002, 2003) whose concern was to distinguish between the conditions which lead to the formation of large-amplitude "table-top" waves, and those conditions which lead instead to wave breaking and the consequent formation of large-amplitude solitary waves with recirculating cores. In a similar vein Vlasenko and Hutter (2002) used numerical simulations of the full Euler equations to study the breaking of internal solitary waves over a slope-shelf configuration appropriate for the Andaman and Sulu seas. Recently Vlasenko and Stashchuk (2006) examined the adiabatic deformation of small-amplitude internal waves over topography in the presence of a (conservative, that is $\nu = 0$) barotropic current, again using numerical simulations of the full Euler equations.

We acknowledge support from INTAS project, 06-1000013-9236, and from RFBR, 06-05-64232, for Talipova.

References

[1] Apel J R, (1995) Linear and nonlinear internal waves in coastal and marginal seas. In: Oceanographic Application of Remote Sensing, (ed) Ikeda M and Dobson F , CRC Press, Boca Raton, Florida, 57-78.

[2] Benney D J (1966) Long non-linear waves in fluid flows. *J. Math. Phys.*, 45: 52-63.

[3] Boussinesq M J (1871) Theórie de l'intumescence liquide appellée onde solitaire ou de translation, se propageant dans un canal rectangulaire. *Comptes Rendus Acad. Sci (Paris)*, 72: 755-759.

[4] Cai, S, Long, X and Gan, Z (2002) A numerical study of the generation and propagation of internal solitary waves in the Luzon Strait. *Oceanologica Acta*, 25: 5160.

[5] Clarke S, Grimshaw R, Miller P, Pelinovsky E and Talipova T (2000) On the generation of solitons and breathers in the modified Korteweg-de Vries equation. *Chaos*, 10: 383-392.

[6] Djordjevic, V and Redekopp, L (1978) The fission and disintegration of internal solitary waves moving over two-dimensional topography. *J. Phys. Ocean.*, 8: 10161024.

[7] Drazin, P G. and Johnson, R. S. (1989) Solitons: an Introduction. CUP, Cambridge, 1989.

[8] Duda, T F, Lynch, J F, Irish, J D, Beardsley, R C, Ramp, S R, Chiu, C-S, Tang, T Y and Yang, Y-J (2004). Internal tide and nonlinear internal wave behavior at the continental slope in the northern south China Sea. *IEEE J. Oceanic Eng.* 29: 1105-1130.

[9] Egorov, Yu A (1993) Evolution of long nonlinear gravity waves on shelves. *Int. J. Offshore and Polar Eng.*, 3: 1-6.

[10] El G A and Grimshaw R (2002) Generation of undular bores in the shelves of slowly-varying solitary waves. *Chaos*, 12: 1015-1026.

[11] Grimshaw, R (1979) Slowly varying solitary waves. I Korteweg-de Vries equation. *Proc. Roy. Soc.*, 368A: 359-375.

[12] Grimshaw R (1981) Evolution equations for long nonlinear internal waves in stratified shear flows. *Stud. Appl. Math.*, 65:, 159-188.

[13] Grimshaw, R (1984) Wave action and wave-mean flow interaction, with application to stratified shear flows. *Ann. Rev. Fluid Mechanics*, 16: 11-43.

[14] Grimshaw R (2001) Internal solitary waves. In: Environmental Stratified Flows, (ed) Grimshaw R (Kluwer, Boston, Chapter 1: 1-28.

[15] Grimshaw R (2005) Korteweg-de Vries equation. In: Nonlinear waves in fluids: Recent advances and modern applications, CISM Courses and Lectures No. 483, Springer, Wien New York, (ed) Grimshaw R, Springer, Wien New York, Chapter 1: 1-28.

[16] Grimshaw R and Mitsudera H (1993) Slowly-varying solitary wave solutions of the perturbed Korteweg-de Vries equation revisited. *Stud. Appl. Math.*, 90: 75-86.

[17] Grimshaw R, Pelinovsky E and Talipova T (1998a) Solitary wave transformation due to a change in polarity. *Stud. Appl. Math.*, 101: 357-388.

[18] Grimshaw, R, Ostrovsky, L A, Shrira, V I and Stepanyants, Yu A (1998b) Nonlinear surface and internal gravity waves in a rotating ocean. *Surveys in Geophysics*, 19: 289-338.

[19] Grimshaw R, Pelinovsky E and Talipova T (1999) Solitary wave transformation in a medium with sign-variable quadratic nonlinearity and cubic nonlinearity. *Physica D*, 132: 40-62.

[20] Grimshaw, R, Pelinovsky, E and Talipova, T (2003) Damping of large-amplitude solitary waves. *Wave Motion*, 37: 351-364.

[21] Grimshaw, R H J and Pudjaprasetya, S R (2004). Generation of secondary solitary waves in the variable-coefficient Korteweg-de Vries equation. *Stud. Appl. Maths*, 112: 271-279.

[22] Grimshaw R, Pelinovsky E, Talipova T and Kurkin A (2004) Simulation of the transformation of internal solitary waves on oceanic shelves. *J. Phys. Ocean.*, 34: 2774-2779.

[23] Grimshaw, R., Pelinovsky, E., Stepanyants, Y and Talipova, T (2006) Modeling internal solitary waves on the Australian North West Shelf. *Marine and Freshwater Research*, 57: 265 272.

[24] Helfrich, K R and Melville, W K (2006) Long nonlinear internal waves. *Ann. Rev. Fluid Mechanics*, 38: 395-425.

[25] Holloway P, Pelinovsky E, Talipova T and Barnes B (1997) A nonlinear model of the internal tide transformation on the Australian North West Shelf. *J. Phys. Ocean.*, 27: 871 - 896.

[26] Holloway P, Pelinovsky E and Talipova T (1999) A generalised Korteweg-de Vries model of internal tide transformation in the coastal zone. *J. Geophys. Res.*, 104: 18333 - 18350.

[27] Holloway P, Pelinovsky E and Talipova T (2001) Internal tide transformation and oceanic internal solitary waves. In: Environmental Stratified Flows, (ed) Grimshaw R (Kluwer, Boston, Chapter 2: 29-60).

[28] Hsu, M-K, Liu, A K and Liu C (2000) A study of internal waves in the China Seas and Yellow Sea using SAR *Cont. Shelf Res.*, 20: 389-410.

[29] Ivanov, V A, Pelinovsky, E N, Talipova, T G and Troitskaya, Yu I (1994) Statistical estimates of the parameters of nonlinear long internal waves off the South Crimea in the Black Sea. *Physical Oceanography*, 6: 253 262.

[30] Johnson, R S (1972) Some numerical solutions of a variable-coefficient Korteweg-de Vries equation (with applications to solitary wave development on a shelf), *J. Fluid Mech.*, 54: 81 - 91

[31] Johnson, R S (1973a) On an asymptotic solution of the Korteweg-de Vries equation with slowly varying coefficients, *J. Fluid Mech.*, 60: 813 - 824144

[32] Johnson R S (1973b) On the development of a solitary wave moving over an uneven bottom. *Proc. Camb. Phil. Soc.*, 73: 183-203.

[33] Korteweg D J, and de Vries H (1895) On the change of form of long waves advancing in a rectangular canal, and on a new type of long stationary waves. *Philosophical Magazine*, 39: 422-443.

[34] Lamb, K G (2003) A numerical investigation of solitary internal waves with trapped cores formed via shoaling. *J. Fluid Mech.*, 451: 109-144.

[35] Lamb, K G (2003) Shoaling solitary internal waves: on a criterion for the formation of waves with trapped cores. *J. Fluid Mech.*, 478: 81-100.

[36] Lamb, K G, and Yan, L (1996) The evolution of internal wave undular bores: comparisons of a fully nonlinear numerical model with weakly nonlinear theory *J. Phys. Ocean.*, 26: 2712-2734.

[37] Lee, C Y and Beardsley, R C (1974) The generation of long nonlinear internal waves in a weakly stratified shear flow. *J.Geophys, Res.,* 79: 453-462.

[38] Levitus S and Boyer T (1994) Climatological Atlas of the World Ocean 1994. U.S.Department of Commerce, NOAA.

[39] Liu, A K (1988) Analysis of nonlinear internal waves in the New York Bight. *J. Geophys. Res.*, 93: 12 317-12 329.

[40] Liu, A K, Chang, Y S, Hsu, M-K and Liang, N K (1998) Evolution of nonlinear internal waves in the East and South China Seas. *J. Geophys, Res.*, 103: 7995-8008.

[41] Liu, A K, Ramp, S R, Zhao, Y and Tswen Yung Tang, T Y (2004) A case study of internal solitary wave propagation during ASIAEX 2001. *IEEE J. Oceanic Eng.* 29: 1144-1156.

[42] Maslowe S A and Redekopp, L G (1980) Long nonlinear waves in stratified shear flows. *J. Fluid Mech.*, 101: 321-348.

[43] Nakoulima, O, Zahibo, N, Pelinovsky, E., Talipova, T, Slunyaev, A and Kurkin, A (2004) Analytical and numerical studies of the variable-coefficient Gardner equation. *Appl. Math. Comp.*, 152: 449-471.

[44] Orr, M H and Mignerey, P C (2003) Nonlinear internal waves in the South China Sea: Observation of the conversion of depression internal waves to elevation internal waves. *J. Geophys. Res.*, 108: No C3, pp 9-1.

[45] Ostrovsky, L A (1978) Nonlinear internal waves in rotating fluids. *Oceanology,* 18: 181-191.

[46] Ostrovsky L A and Pelinovsky EN (1970) Wave transformation on the surface of a fluid of variable depth. *Akad. Nauk SSSR, Izv. Atmos. Ocean Phys.*, 6: 552-555.

[47] Pelinovsky D and Grimshaw R H J (1997) Structural transformation of eigenvalues for a perturbed algebraic soliton potential. *Phys. Lett. A*, 229: 165-172.

[48] Pelinovsky, E, Talipova, T and Ivanov, V (1995) Estimations of nonlinear properties of internal wave field off the Israel coast. *Nonlinear Processes in Geophysics*, 2: 80 - 88.

[49] Poloukhina, O. , Poloukhin, N., Talipova, T., Pelinovsky, E., Grimshaw, R., Lamb K. and Muyakshin, S. (2002). Modelling of large-amplitude internal waves in the ocean. *Proceedings of the International Conference dedicated tp the 100th anniversary of A.A. Andronov; "Progress in Nonlinear Science, Volume II, Frontiers of Nonlinear Physics, ed. A.G. Litvak, Inst. Applied Physics, Nizhny Novgorod*, 252-257.

[50] Poloukhin, N V, Talipova, T G, Pelinovsky, E N and Lavrenov, I V (2003) Kinematic characteristics of the high-frequency internal wave field in the Arctic Ocean. *Oceanology*, 43: 356-367.

[51] Poloukhin, N V, Pelinovsky, E N, Talipova, T G and Muyakshin, S I (2004) On the effect of shear currents on the vertical structure and kinematic parameters of internal waves. *Oceanology*, 44: 22-29.

[52] Ramp, S R, Tang, T Y, Duda, T F, Lynch, J F, Liu, A K, Chiu, C-S, Bahr, F L, Kim, H-R and Yang, Y-J (2004) Internal solitons in the northeastern South China Sea. Part I: sources and deep water propagation *IEEE J. Oceanic Eng.* 29: 1157-1181.

[53] Rayleigh J W S (1876) On waves. *Phil. Mag.*, 1: 257-279.

[54] Russell J S (1844) Report on Waves 14th meeting of the British Association for the Advancement of Science, 311-390.

[55] Salusti, F, Lascaratos, A, and Nittis K (1989) Changes of polarity in marine internal waves: Field evidence in eastern Mediterranean Sea. *Ocean Modelling*, 82: 10-11.

[56] Small, J (2001a) A nonlinear model of the shoaling and refraction of interfacial solitary waves in the ocean. Part I: Development of the model and investigations of the shoaling effect. *J. Phys. Ocean.*, 31: 31633183.

[57] Small, J (2001b) A nonlinear model of the shoaling and refraction of interfacial solitary waves in the ocean. Part II: Oblique refraction across a continental slope and propagation over a seamount. *J. Phys. Ocean.* , 31: 31843199.

[58] Small, J. (2003) Refraction and shoaling of nonlinear internal waves at the Malin Shelf Break. *J. Phys. Ocean.*, 33: 2657- 2674.

[59] Small, R J and Hornby, R P (2005) A comparison of weakly and fully non-linear models of the shoaling of a solitary internal wave *Ocean Modelling* 8: 395416.

[60] Talipova, T, Pelinovsky, E and Kouts, T (1998) Kinematic characteristics of an internal wave field in the Gotland Deep in the Baltic Sea. *Oceanology*, 38: 33 - 42.

[61] Tappert, F D and Zabusky, N J (1971) Gradient-induced fission of solitons *Phys. Rev. Lett.* 27: 1774 - 1776.

[62] Tung, K K, Ko, D R S and Chang, J J (1981) Weakly nonlinear internal waves in shear. *Stud. Appl. Math.*,65: 189-221.

[63] Vlasenko, V and Hutter , K (2002) Numerical experiments on the breaking of solitary internal waves over a slopeshelf topography. *J. Phys. Ocean.*, 32: 1779-1793.

[64] Vlasenko, V and Stashchuk, N (2006) Amplification and suppression of internal waves by tides over variable bottom topography. *J. Phys. Ocean.*, 36: 1959-1973.

[65] Yang, Y-J, Tang, T Y, Chang, M H, Liu, A K, Hsu, M-K and Ramp, S R (2004) Solitons northeast of Tung-Sha Island during the ASIAEX pilot studies. *IEEE J. Oceanic Eng.*, 29: 1182-1199.

[66] Zheng, Q, Klemas, V, Yan X-H and Pan, J (2001) Nonlinear evolution of ocean internal solitons propagating along an inhomogeneous thermocline. *J. Geophy. Res.*, 106: 14083-14094.

[67] Zheng, Q, Klemas, V, Zheng, Q and Yan X-H (2003) Satellite observation of internal solitary waves converting polarity *Geophys. Res. Lett.*, 30: No. 19, pp 4-1.

[68] Zhou, X and Grimshaw, R (1989) The effect of variable currents on internal solitary waves. *Dyn. Atmos. Oceans.*, 14: 17-39.